Supplemental Materials

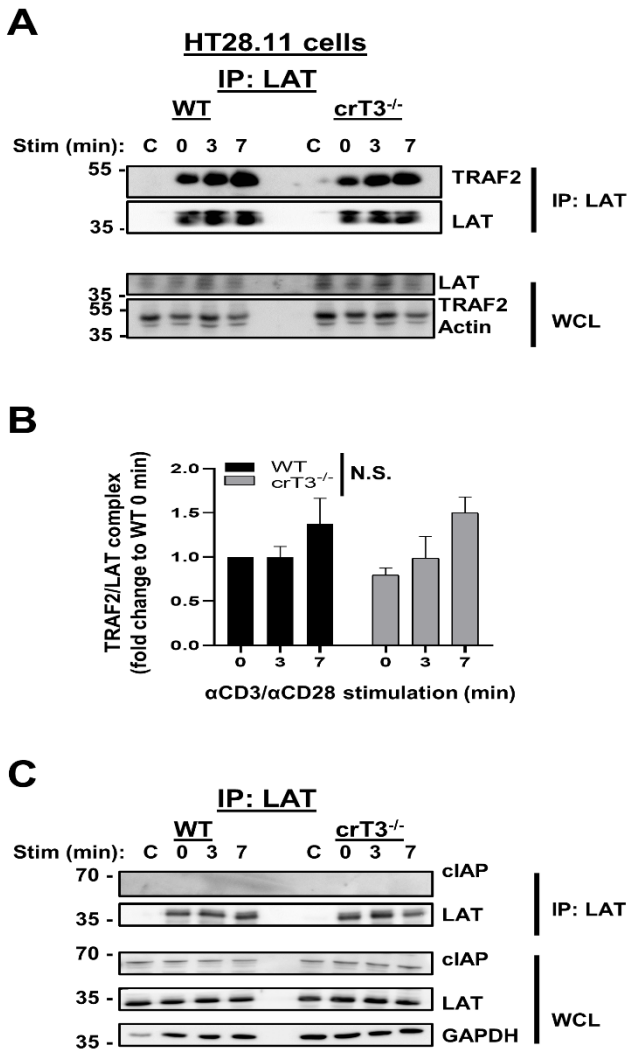

Supplemental figure 1. Association of TRAF2 with the LAT complex.

A) Human HT28.11 T cells were stimulated through CD3/CD28 for the times indicated and lysed, and LAT was immunoprecipitated. Association of TRAF2 with the LAT complex was assessed by WB. Blots are representative of 3 independent experiments. B) Densitometric analysis of the ratio of TRAF2 associated with the LAT complex at each timepoint shown in A, with each timepoint normalized to WT 0 min, to determine the impact of genotype on the kinetics of the TRAF2-LAT association. The difference in TRAF2/LAT complex association between WT and crT3$^{-/-}$ cells was not statistically significant. C) HT28.11 (human) T cells were stimulated as in A, and LAT was immunoprecipitated. Association of cIAP1/2 with the LAT complex was assessed by WB. Blots are representative of 3 independent experiments. 'C' indicates samples that only received stimulatory Abs, i.e. no IP Abs added after lysis (A, C). Graph depicts mean ± SEM. A 2-way ANOVA was performed to establish statistical significance in B. The reference group used to calculate fold change was not included in the analysis. 'N.S.': not significant.

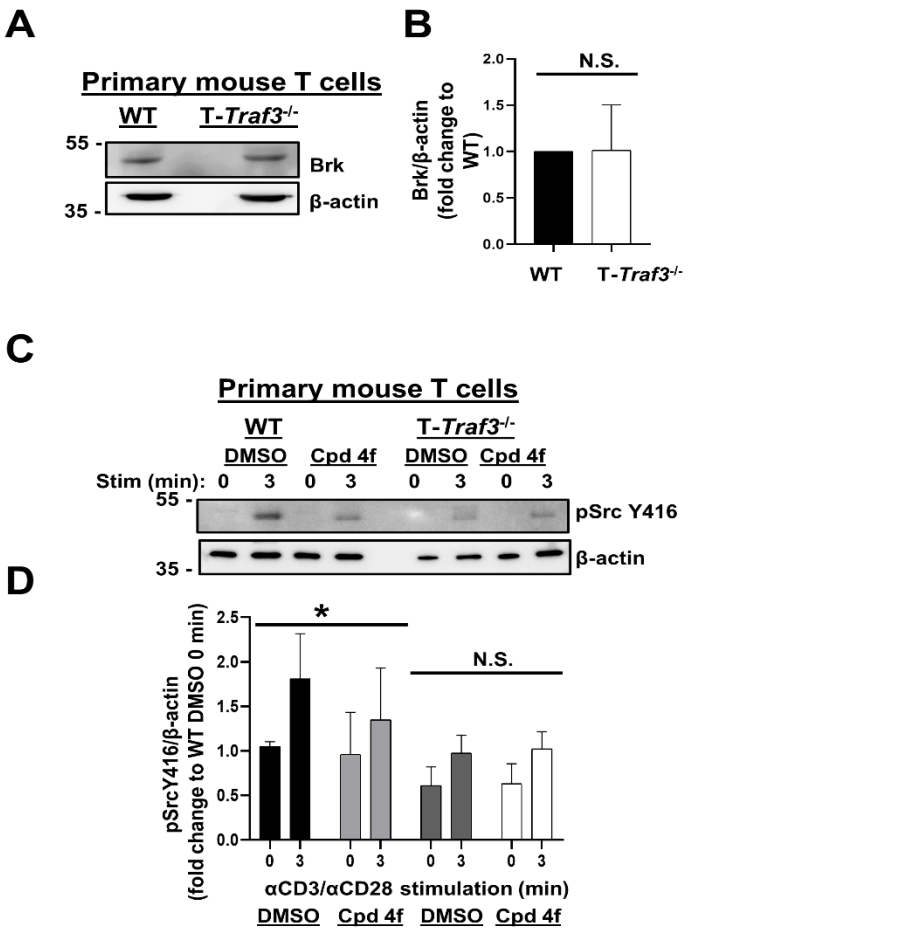

Supplemental figure 2. Role of Brk in primary mouse T cells.

Primary mouse T cells were isolated from WT and T-*Traf3*$^{-/-}$ mice as described in Materials and Methods. A) Expression of Brk in WCL from unstimulated primary mouse T cells was assessed by WB. Blots are representative of 3 independent experiments. B) Densitometric analysis of the ratio of abundance of Brk to that of β-actin, with the ratio of Brk to β-actin in WT T cells set as 1. The difference in Brk expression between WT and T-*Traf3*$^{-/-}$ cells was not statistically significant by unpaired t-test. C) WT and T-*Traf3*$^{-/-}$ primary mouse T cells were treated with DMSO or the Brk inhibitor Cpd 4f for 2 hours, as described in Materials and Methods, then stimulated through CD3/CD28 for the times indicated and lysed. Phosphorylation of Fyn at Y^{416} and Src at Y^{394} was detected by WB with an anti-pSrcY^{416} Ab. Blots are representative of 4 independent experiments. D) Densitometric analysis of the ratio of abundance of pSrc Y^{416} to that of β-actin. Fold change was calculated by dividing the ratio of pSrc Y^{416}/β-actin in each lane to the ratio of pSrc Y^{416}/ β-actin for DMSO-treated WT 0 min, to determine the impact of Cpd 4f treatment on Src kinase activation relative to a baseline value. The difference between DMSO-treated and Cpd 4f-treated WT cells was statistically significant (*p=0.0177). The difference between DMSO-treated and Cpd 4f-treated T-*Traf3*$^{-/-}$ cells was not statistically significant. Graphs depict mean ± SEM. A 2-way ANOVA was performed to establish statistical significance in C. The reference group used to calculate fold change was not included in the analysis. *: $p<0.05$; 'N.S.': not significant.

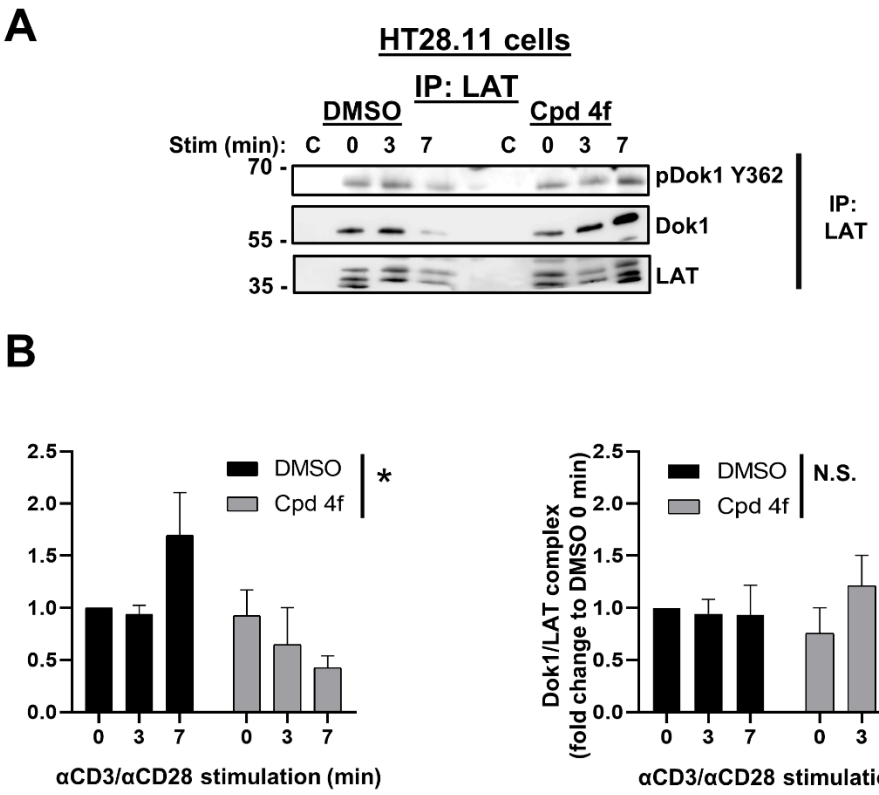

Supplemental figure 3. Impact of Brk inhibition on activity of Dok1 associated with the LAT complex.

A) Human HT28.11 WT T cells were treated with DMSO or the Brk inhibitor Cpd 4f for 2 hours as described in Materials and Methods, then stimulated through CD3/CD28 for the times indicated and lysed. LAT was immunoprecipitated, and association of pDok1 Y^{362} and total Dok1 with the LAT complex was assessed by WB. Blots are representative of 4 independent experiments. B) Densitometric analysis of the ratio of pDok1 Y^{362} associated with Dok1 (left) and the ratio of Dok1 associated with the LAT complex (right) at each timepoint shown in A, with each timepoint normalized to DMSO 0 min. The difference in pDok1 Y^{362}/Dok1 association between DMSO-treated and Cpd 4f-treated WT cells over time was statistically significant (*p=0.0177). The difference in Dok1/LAT complex association between DMSO-treated and Cpd 4f-treated cells was not statistically significant. * in IP indicates a band from the molecular weight (MW) ladder loaded in that lane. 'C' indicates samples that only received stimulatory Abs (A). Graph depicts mean ± SEM. A 2-way ANOVA was performed to establish statistical significance in B. The reference group used to calculate fold change was not included in the analysis. *: $p<0.05$; 'N.S.': not significant.

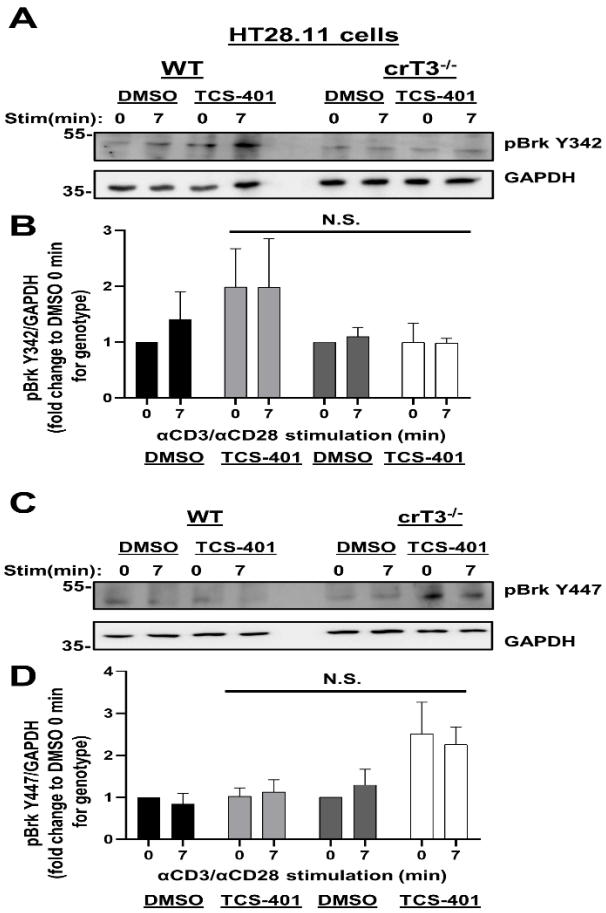

Supplemental figure 4. Impact of PTP1B inhibition on phosphorylation of Brk.

A) Human HT28.11 WT and crTRAF3$^{-/-}$ T cells were treated with DMSO or the PTP1B inhibitor TCS-401 for 2 hours as described in Materials and Methods, then stimulated through CD3/CD28 for the times indicated and lysed. Phosphorylation of Brk at Y^{342} was assessed by WB. Blots are representative of 3 independent experiments. B) Densitometric analysis of the ratio of abundance of pBrkY^{342} to that of GAPDH in each lane. Fold change was calculated by dividing the ratio of pBrkY^{342}/GAPDH at each timepoint by the ratio of pBrk Y^{342}/GAPDH at the DMSO 0 min timepoint for each cell line, to control for cell line-specific differences in abundance of pBrk Y^{342}. The difference in pBrk Y^{342} abundance between WT and crTRAF3$^{-/-}$ cells treated with Cpd 4f was not statistically significant. C) Human HT28.11 WT and crTRAF3$^{-/-}$ T cells were treated as described in Supp. Fig. 4A. Phosphorylation of Brk at Y^{447} was assessed by WB. Blots are representative of 4 independent experiments. D)Densitometric analysis of the ratio of abundance of pBrkY^{447} to that of GAPDH in each lane. Fold change was calculated by dividing the ratio of pBrkY^{447}/GAPDH at each timepoint by the ratio of pBrk Y^{447}/GAPDH at the DMSO 0 min timepoint for each cell line, to control for cell line-specific differences in abundance of pBrk Y^{447}. The difference in pBrk Y^{447} abundance between WT and crTRAF3$^{-/-}$ cells treated with TCS-401 was trending toward statistical significance (p=0.0677). Graphs depict mean ± SEM. A 2-way ANOVA was performed to establish statistical significance in B and D. The reference group used to calculate fold change was not included in the analysis. 'N.S.': not significant.